Soft Matter

Accepted Manuscript

ROYAL SOCIETY OF CHEMISTRY

www.rsc.org/softmatter

Soft Matter

ARTICLE

Are polymers glassier upon confinement?

J. Spièce[a], D. E. Martínez-Tong[b,c], M. Sferrazza[b], A. Nogales[c] and S. Napolitano[a,*]

Received 00th January 20xx,
Accepted 00th January 20xx

DOI: 10.1039/x0xx00000x

www.rsc.org/

Glass forming systems are characterized by a stability against crystallization upon heating and by the easiness with which their liquid phase can be tranformed into a solid lacking of long-range order upon cooling (glass forming ability). Here, we report the thickness dependence of the thermal phase transition temperatures of poly(L-lactide acid) thin films supported onto solid substrates. The determination of the glass transition, cold crystallization and melting temperatures down to a thickness of 6 nm, permitted us to build up parameters describing glass stability and glass forming ability. We observe a strong influence of the film thickness on the latter, while the former is not affected by 1D confinement. Further experiments permitted us to highlight key structural morphology features giving insights to our ellipsometric results via a physical picture based on the changes in the free volume content in proximity of the supporting interfaces.

1. Introduction

The molecular mechanisms governing vitrification, the process preventing crystallization of a liquid upon cooling or pressurizing, are still not clear[1]. The liquid to glass transition is, actually, one of the most debated through the unsolved problems of condensed matter,[2-4] having a large number of practical implications. Vitrification, in fact, strongly affects the processing of soft materials: owing to weak interaction potentials on the order of thermal fluctuations, many polymers, liquid crystals, biological molecules and colloids do not crystallize easily[5].

A well-established methodology to investigate vitrification is the determination of phase transition temperatures occurring to a non-crystalline solid during a heating process, namely the glass transition (T_g), cold crystallization[6] (T_{CC}) and melting (T_m) temperatures[7]. The combination of these quantities permits, in fact, to characterise parameters such as the glass forming ability (GFA, ~ T_g/T_m), that is, the easiness with which a liquid can be converted into a glass circumventing crystallization, and the glass stability (GS, ~ T_{CC} - T_g) that opposes crystallization upon heating. Systematic analysis of these parameters allows the identification of the best formulation for glasses and their processing conditions[8, 9].

Considering the enormous and growing interest towards soft matter, especially polymers, in thin film geometry – for example for the development of nanodevices, coatings, conducting polymer devices, *etc.* – an evaluation of the glass forming ability and stability in confined geometries (< 100 nm) is urgently required[10]. In particular, we should focus on questions of the type: *are glasses more stable at the nanoscale level? Is it easier to vitrify soft matter in confined geometries?*

In this paper, exploiting the sensitivity of ellipsometry, we present a study on the glass transition, cold crystallization and melting of thin films of poly(L-lactide) (PLLA), which permitted to investigate the thickness dependence of the GS and GFA of this biodegradable polymer, down to few nm. Our investigation revealed that, while the glass stability is not particularly affected by the reduction of the sample dimension, thinner films show a particularly enhanced glass forming ability. Complementary studies, performed via Atomic Force Microscopy and Small Angle X-ray Scattering, allowed us to disentangle the origin of the confinement effects on T_g, T_{CC} and T_m, and to propose a physical picture based on the changes in the free volume content in proximity of the supporting interfaces.

2. Experimental

2.1 Materials and Methods

PLLA (M_w = 67,000 g/mol, PDI < 1.4, Sigma-Aldrich) was used as received. Thin films were prepared by spin coating solutions of the polymer in chloroform (1 min, 3000 rpm) onto two different types of substrates: a) silicon wafers covered by a native oxide layer (~ 2 nm); b) ~ 150 nm thick thermally

[a] Laboratory of Polymer and Soft Matter Dynamics, Faculté des Sciences, Université Libre de Bruxelles (ULB), Boulevard du Triomphe, 1050 Bruxelles, Belgium
[b] Département de Physique, Faculté des Sciences, Université Libre de Bruxelles (ULB), Boulevard du Triomphe, 1050 Bruxelles, Belgium.
[c] Instituto de Estructura de la Materia (IEM-CSIC). C/ Serrano 121, Madrid 28006, Spain.
* snapolit@ulb.ac.be

Electronic Supplementary Information (ESI) available: [details of any supplementary information available should be included here]. See DOI: 10.1039/x0xx00000x

evaporated aluminum layers, prepared under vacuum (< 10^{-6} mbar) onto the above-mentioned Si wafers (exposure to air resulted in the formation of a native oxide layer of ~ 3 nm). Polymer films of different thicknesses (h), between 150 nm to 6 nm, were obtained by controlling by the concentration of the solutions used for spin coating. Before measurements, samples were annealed for 30 s at 453 K (> 433 K, the bulk melting temperature determined by differential scanning calorimetry (DSC)), and quenched (~ 100 K/s) onto a cold plate (273 K). This procedure successfully avoided the formation of crystalline structures, as confirmed by X-ray scattering.

The ellipsometric angles Δ and Ψ were recorded via a spectroscopic ellipsometer (MM16-Horiba), with a wavelength range λ = 430 – 850 nm. Samples were placed on a Linkam stage, located on the ellipsometer goniometer, allowing a fine temperature control. To ensure homogeneous temperature before the onset of the measurement, samples were kept at 303 K for 5 min. This annealing step was followed by a 2 K/min heating ramp up to 453 K, to characterize phase transitions upon heating.

To study the crystalline morphology of the thin films, we carried out AFM measurements using a Multimode 8 microscope, equipped with a Nanoscope V controller (Bruker). Topography measurements were taken using the amplitude modulation tapping protocol, with NSG30 probes (NT-MDT). AFM topography images were analyzed via Nanoscope 1.50 (Bruker). Thickness of the polymer films was also determined by AFM, quantifying the step between the silicon and polymer surface, after scratching the polymer surface, with sharp tweezers. Small Angle X-ray Scattering (SAXS) measurements were carried out using a Bruker AXS Nanostar X-ray scattering spectrometer, using Cu K_α radiation (λ = 0.154 nm) tube.

Irreversible adsorption was studied by reproducing Guiselin's experiment[11], via the same protocol as Housmans *et al.*[12]. In order to determine the thickness of the layer of PLLA irreversibly adsorbed onto the supporting substrate (h_{ads}), we annealed 30 nm-thick films at 373 K for different times. Samples were then soaked in chloroform for 20 min to dissolve the unabsorbed polymer chains and, after drying, the value of h_{ads} at ambient conditions was determined by ellipsometry.

2.2 Identifying phase transitions in the temperature dependence of the ellipsometric angles

Temperature-dependent ellipsometry measurements[13-15], allowed detecting phase transitions in PLLA films as thin as 6 nm. Focusing on the thickest samples, the transitions in the ellipsometric angles occur in proximity of the values of the glass transition (T_g), cold crystallization (T_{CC}) and melting temperature (T_m) found by differential scanning calorimetry operated in comparable experimental conditions.

To achieve quantitative analysis of our data, we considered the changes in the macromolecular structure during the phase transitions commonly observed in semicrystalline polymers, and their impact on the optical properties of nanometer-sized samples. In the case of homogenous thin films (*e.g.* amorphous systems, at temperatures < T_{CC}), T_g can be studied by measuring the temperature dependence of the ellipsometric angles; in the following discussion we will refer to Ψ, although similar arguments can be applied to Δ.

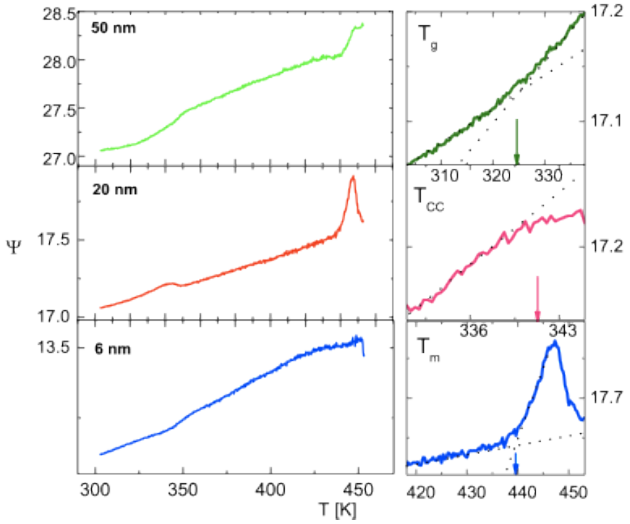

Figure 1. Left panels: temperature dependence of the ellipsometric angle Ψ for films of PLLA of different thicknesses, deposited on silicon oxide. Right panels: an exampl the determination of the phase transition temperatures, following the procedure indicated in section 2.2, is given for the 20 nm thick sample.

Because of the linear dependence of Ψ on h in the thickness range studied, the condition $\delta|h| \sim \delta|\Psi|$ is valid, where δ indicates a small increment of the quantity[16]. Furthermore, assuming that the constraints at the supporting interface allow thermal expansion only in the normal direction[17], it holds that $h(T) \sim V(T)$, where V is the volume of the sample. Upon heating, molecular mobility increases and the structural α–modes responsible for the glass transition get faster[5]. Indicating with τ the characteristic time of these modes, T_g is achieved when we can no longer neglect the relative variation in relaxation time during a time in the order of τ, that is, $\tau\partial(\ln\tau^{-1})/\partial t \sim 1$. The material softens in proximity of this temperature, which results in a neat increase in thermal expansion, $\sim \partial V/\partial T$. Because this quantity is directly proportional to the temperature derivative of the ellipsometric angles, we identify T_g as the transition temperature in between the two linear regimes in $\Psi(T)$. Following standard fitting procedures, the glass transition temperature was attributed to the crossing of linear regressions in the glassy and in the supercooled liquid state; fitting with functions mimicking smooth transitions provided similar results.[18]

At temperatures much higher than T_g we observed a systematic deviation from the linear trends in $\Psi(T)$. We attributed the cause of this phenomenon to the formation of ordered structures during cold crystallization. Because of the different refractive index in the crystalline domains, at $T > T_{CC}$ the system becomes optically heterogeneous and the linear relation between sample thickness and ellipsometric angles no longer holds. Roughness development on the surface, connected to the formation of crystalline structures, plays also a role for this deviation. Consequently we assigned T_{CC} to the temperature where the departing from the linear trend in the

temperature dependence of the ellipsometric angles exceeded 3 standard deviations. Finally, following similar arguments on the change in the heterogeneous character of our films upon the conversion of crystals into the equilibrium liquid phase, we could identify the melting transition as an abrupt change in $\Psi(T)$ occurring at $T > T_{CC}$. In the next sections we will discuss the thickness dependence of the different phase transitions.

3. Results and discussion

3.1 Glass transition

Figure 2a shows the values of the glass transition temperature of thin films of PLLA of different thicknesses, deposited on different substrates, see caption for a legend. For films thicker than 20 nm, we determined T_g = 329 ± 2 K, in line with what reported for bulk PLLA[19-21]. Below this threshold thickness, the value of T_g smoothly increased, reaching a shift with respect to the bulk value T_g^0 ($\Delta T_g = T_g - T_g^0$) of +8 K for 8 nm thick films on SiO_2. Due to low signal/noise ratio, we could not detect a glass transition for films deposited on Al thinner than 16 nm.

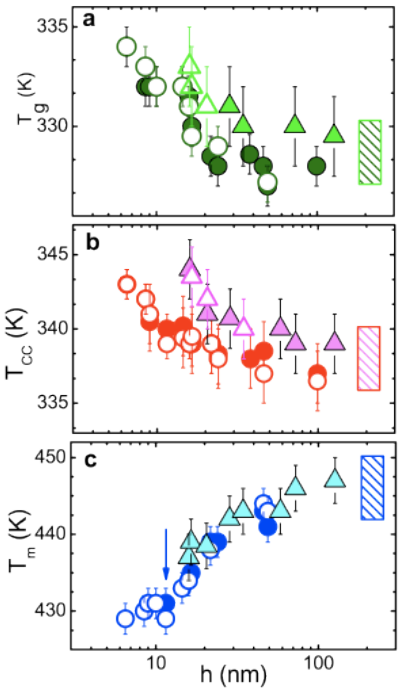

Figure 2. Thickness dependence of the (a) glass transition temperature (T_g), (b) cold crystallization temperature (T_{cc}) and (c) melting temperature (T_m), as obtained from the analysis of the temperature dependence of the ellipsometric angles Δ (open symbols) and Ψ (closed symbols). Results for silicon oxide (circles) and aluminum (triangles) substrates are presented simultaneously. T_m results on Al show only the Ψ ellipsometric angle, since the temperature dependence of Δ was excessively noisy.

Shifts in the glass transition temperature upon confinement have been widely reported for a large number of polymers[22-28]. The condition $\Delta T_g < 0$ is often observed and usually explained in terms of faster dynamics at the free surface or packing frustration at the adsorbing interface. On the contrary, trends similar to that of PLLA ($\Delta T_g > 0$) are less common in the case of supported films but often found for capped films (no free surfaces) and nanocomposites. Focusing on supported films, Wang *et al.*[29] found ΔT_g > 10 K for 10 nm-thin films of poly(bisphenol A hexane ether), Erber *et al.*[30] observed a similar raise for films of different polyester architectures, while Tate *et al.*[31] found ΔT_g > 60 K for poly(4-hydroxystyrene) films grafted on silicon oxide substrates. We might be tempted to explain these results in terms of slower segmental mobility at the supporting interface. This idea would be further confirmed via broadband dielectric spectroscopy measurements by Vanroy *et al.*[32], where the value of τ of thin films of PLLA capped between Al layers, increased by 5 folds.

Although this conjecture is commonly reported in the literature, recent work[28, 33] indicates that there is no intrinsic correlation between results obtained in equilibrium conditions (*e.g.* recording a dielectric spectrum where the measurement time exceeds by far the relaxation time) and in temperature scans from non-equilibrium to equilibrium and vice versa (e.g. ellipsometric measurements, see the criterion for T_g discussed in 2.2).

For example, films of PS capped into Al layers show a reduction in T_g measured in non-equilibrium/equilibrium scans at invariant segmental mobility, that is, at constant value of the T_g extrapolated from equilibrium measurements. As observed by Cangialosi and coworkers[34], this intriguing feature of glassy dynamics implies that the time scale of equilibration (the one probed in a temperature scan, providing the value of T_g) decouples from the molecular timescale (the one related to spontaneous fluctuations and thus assessed in a relaxation/retardation experiment, ~ τ) upon confinement. This decoupling can be rationalized in terms of the free volume holes diffusion (FVHD) model[35, 36] where – considering a heating scan as in our experiments – T_g is assigned as the temperature at which free volume holes can diffuse sufficiently fast to reach the free surface, within the time scale fixed by the scanning rate. This feature ensures equilibration. The condition $\Delta T_g > 0$ implies that the overall diffusion of free volume holes gets hindered upon confinement. Remarkably, lower diffusion coefficients do not require slower dynamics (larger τ), as verified by experiments of diffusion of probes in ultrathin polymer films[37]. With these ideas in mind, one might argue that higher values of T_g imply smaller diffusion coefficients of free volume holes, *e.g.* because of a more efficient molecular packing in proximity of the adsorbing interface. Within this framework, the increase in T_g in the thinner films would be explained via the increase in volume fraction of adsorbed chains upon reduction of the film thickness. Similarly, we could argue that at constant thickness of the polymer film we should expect higher T_g's in case of more densely packed adsorbed layers. Noteworthy, this trend was previously validated by measurement of the T_g of thin films of PS with different adsorption degrees[38].

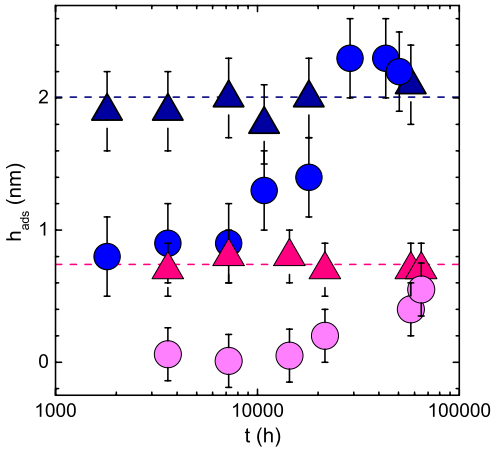

Figure 3. Kinetics of irreversible adsorption of PLLA onto aluminum (blue tones) and silicon (pink tones) at 373K. We performed experiments on both as-casted films (circles) and melt-quenched samples (triangles) prepared in the same annealing conditions used for the films tested by ellipsometry. As the value of h_{ads} for films not processed at $T>T_m$ converges to that of melt-quenched samples, we can discard the occurrence of chain degradation during treatment at high temperatures.

We thus considered the impact of a smaller diffusion coefficient in the adsorbed layer on the overall diffusion time of the free volume holes of the film, t_D, and on ΔT_g. We assumed a temperature dependence of the diffusion coefficients (~ t_D^{-1}) following a super-Arrhenius law and considered the prediction of previous modeling on an analogous system[39]. Under these conditions, a large increase in t_D corresponds to minor shifts in the transition temperatures, that is, a drop of orders of magnitude in t_D^{-1} might result in a T_g increase of a few K. The results in Figure 2a are in line with this reasoning. In fact, T_g occurs at higher temperatures for films deposited on Al, the substrate where 3 folds thicker adsorbed layers were measured, see Figure 3 its caption. We anticipate that the same modeling predicts a similar trend for the shift in cold crystallization temperature; we will return on this point in the next paragraph.

3.2 Cold Crystallization

As temperature is further increased, the chains of PLLA reach sufficient molecular mobility allowing devitrification and formation of ordered structures (cold crystallization). Figure 2b shows the cold crystallization temperature as a function of *h*. For both substrates, an overall increase of T_{CC} is observed upon thickness reduction. Considering that in the regime of cold crystallization the formation of ordered structures is limited by diffusion and incorporation of material at the rate of monomer friction (~ τ^{-1}), the crystallization and the glass transition are intrinsically bound. Fundamental relations of the form $t_C = \tau^{\xi}$, where t_C is a characteristic time for cold crystallization and ξ a positive constant (< 1), were experimentally verified[39-41].
In line with these ideas, following the trend observed for the glass transition, at any thickness devitrification occurs at higher temperatures for PLLA films deposited on Al. The difference between the transition temperatures on the two substrates is further enhanced for the cold crystallization. We argue that this larger confinement effect originate from larger timescales of the crystallization phenomena.

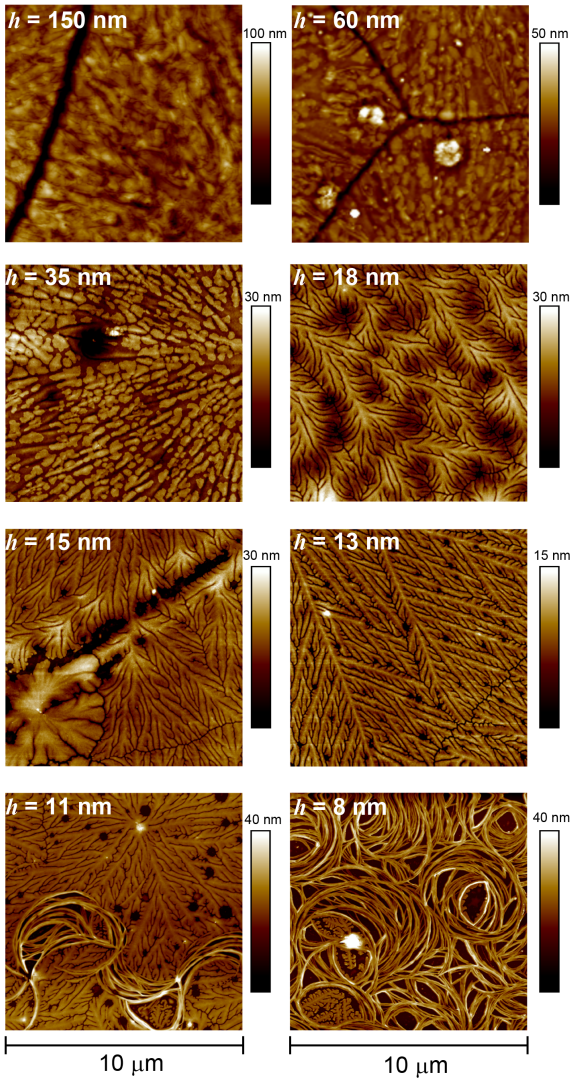

Figure 4. 10x10 μm^2 AFM topography images of PLLA thin films annealed at 373 K for 24 h. Labels indicate the thickness (*h*) of the as casted film.

To better understand the thickness dependence of T_{CC}, we furthermore considered the impact of other relevant factors to the crystallization in 1D confinement. Previous reports have shown that the rate of crystallization decreases significantly upon reducing film thickness, leading to an increase of crystallization time and larger devitrification temperatures[32, 42, 43]. These timescales and rates shifts can be related to temperature and thickness dependence by considering the density of active nuclei in the films[39]. Liu and Chen[42] summarized the possible scenarios of the crystallization kinetics' slowing-down: (1) a reduction of molecular mobility due to an increase of the glass transition temperature of the system, (2) the presence of a reduced mobility layer at the polymer/substrate interface, hypothesis similar to what was discussed above, and (3) the reduction of the number of active nuclei at a reduction of the thickness. Also, Vanroy *et al.* proposed an alternative scenario based on the increase in the

activation energy for the rotational barriers in adsorbed layers yielding a lower growth rate[10]. In order to elucidate which of these factors could be related to the crystallization process in the PLLA under 1D confinement, AFM measurements were performed. This type of analysis, similarly as that of many other nondestructive techniques, is limited to the presence of crystalline structures at the free surface. Regardless of the difficulty in investigating the bulk component, we sought for correlations between structure and dynamics to test the validity of the above-mentioned hypotheses. To achieve this goal, thin films of PLLA were annealed at 358 K, 373 K and 393 K, for 24 h. In all cases, AFM revealed the development of well-organized surface features.

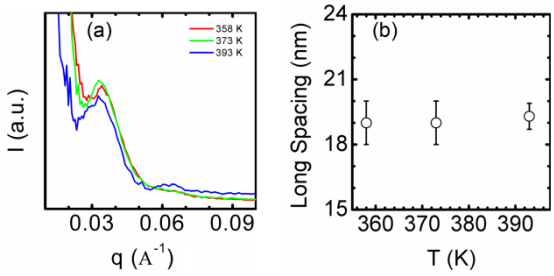

Figure 5. Small Angle X-ray Scattering (SAXS) diffraction patterns for PLLA bulk samples annealed for 24 h at different temperatures. (b) Long-spacing of the PLLA crystals calculated from the maxima around q = 0.035 A^{-1} in figure (a).

Figure 4 shows 10x10 μm^2 AFM topography images of the films annealed at 373 K – the annealing temperature did not affect the morphology of the crystals. Crystalline features are present on the surface of each film investigated, regardless of the film thickness, implying that the annealing time was sufficient to permit nucleation and growth of crystals even in the thinner films. The surface of thick films (h > 35 nm) is covered by spherulites, the same morphology reported for PLLA in bulk[44].
As film thickness was decreased, at h = 18 nm, the crystalline morphology showed a transition to dendritic structures. Dendrites are visible down to h = 13 nm, indicating that this might be the most stable layout of the PLLA crystals in these processing conditions. Previous work verified that polymer dendritic crystals are related to the growth of the polymer chains in a direction normal to the substrate (flat-on lamellae)[45, 46]. This lamellar orientation transition has been previously observed for other polymers[29, 47] and can be related to different factors such as film thickness, polymer/substrate interactions[29, 47, 48] and the influence of the adsorbed polymer chains[49]. In particular, the development of an irreversible adsorbed layer of PLLA onto the supporting substrates (as illustrated in Figure 3) serves as indication of the polymer/substrate interactions. Monte Carlo simulations by Ma *et al.*[48] showed that changes in crystal orientation of polymer thin films could be related to these interactions, concluding that at the interface between a thin film and a sticky wall flat-on crystal growth represents the dominating contribution to the final crystallinity, as in our case.
Finally, in figure 4, the two thinner films (h = 11 and 8 nm) show the development of new crystalline morphology. Besides the flat-on dendritic crystal, we observe curved needle-like structures. These curved crystals have been previously reported for PLLA ultrathin films and related to edge-on lamellae[45, 50], that would appear at very small film thicknesses (around and below 10 nm) and at temperatures well above T_g. Under these conditions, the edge-on lamellae act as secondary nuclei to other edge-on lamellae, leading to U-shaped and loop-shaped structures[45]. Also, the opposing edge-on circular crystals to flat-on dendritic crystals could be linked to dewetting and adsorption. Edge-on crystals growing perpendicular to an induced nucleation zone have been previously reported[51]; thus it is possible to imagine that an induced nucleation zone, such as a circular hole appearing due to dewetting, could give circular shape crystals.
Remarkably the structural transition from spherulitic to denditric morphology takes place at thicknesses comparable to those reported by Vanroy *et al.* for the slowing down in segmental dynamics (increase of T_g) of thin films of PLLA[32]. To unveil the origin of this intriguing correlation between structure and dynamics upon 1D confinement, we performed SAXS measurements, which allows determining the size of long spacing of the polymer, a parameter defined as the average separation between stacked lamellar crystals[52]. 100 μm-thick films were prepared by solvent casting, and annealed for 24 h at 358 K, 373 K and 393 K, prior to the scattering experiment. Figure 5a shows the 1-D diffraction patterns (intensity) vs the scattering vector (q=4π/λsinθ, where λ = 0.154 nm, and θ represents the scattering angle). The intensity show maxima located around q = 0.035 $Å^{-1}$ of comparable intensity in each sample. These peaks are related to the long spacing of the polymer. Independently of the annealing temperature, this length was 19 ± 1 nm, see Figure 5b, a value in agreement the thickness at which the transition in morphology and the onset of slower dynamics take place. Thus, one could consider the development of flat-on crystals as the penalty paid by the polymer in order to remain semi-crystalline at thicknesses below its (bulk) long-range order. Moreover, these new rearrangements affect not only the polymer crystals but also the amorphous chains stacked in-between.

3.3 Melting

Regardless of the supporting substrate, T_m decreases as a function of h^{-1} down to the threshold thickness h_c= 12 ± 2 nm. This value is highlighted in figure 2c by an arrow. Below h_c we observed a constant value of T_m = 430 ± 2 K ($T_m(h_c)$ / T_m (bulk) ≈ 0.95). Analysis of previous works[13, 53-56] on relatively thick films, support similar scaling of T_m with h^{-1} resembling the classical Gibbs-Thomson equation, written for the shift in melting temperature of spheres of radius r, as $\Delta T_m = 4T_m^{\infty}\gamma_{SL}(\Delta H_f\ \rho\ r)^{-1}$, where T_m^{∞} indicates the bulk transition temperature, γ_{SL} is the solid/liquid interfacial energy, ΔH_f the bulk enthalpy of fusion and ρ the density of the solid phase. The use of such a formalism in thin films requires assuming that $h \sim r$, which is in disagreement with the h-invariant T_m below h_c. On the other hand, extensive investigation of the melting transition via scanning probe microscopy indicated

that in the case of supported films the energy gain upon adsorption should be also considered. Consequently, the term ΔH_f should be replaced by $\Delta H_f (1-\phi) + \Delta H_a \phi$, where ϕ indicates the fraction of polymers which is adsorbed onto the supporting substrate[53, 57]. This adjustment seems inadequate in explaining the constant T_m value for the thinnest films, because it would require a very unlikely combination of factors, and a thickness dependent ϕ. Moreover, density might change in proximity of the solid interface.

Due to the above-mentioned difficulties in univocally determining the absolute values of its variables, we preferred not continuing our analysis based on the classical formulation the Gibbs-Thomson equation. On the contrary, we opted for a generalized equation of the form $\Delta T_m = k_{GT}/x$, where k_{GT} is a term taking into account the confining geometry and the previously mentioned quantities, and x indicates the confining dimension affecting the depression in T_m. We thus supposed that the latter quantity is given by the maximum size achieved by the crystalline fraction upon prolonged annealing ($h_{crys} \sim x$), a value estimated as the thickness of the film after annealing via AFM, see details in the caption of Figure 6; in the same plot we compared h_{crys} and the thickness of the amorphous films (h_{amor}).

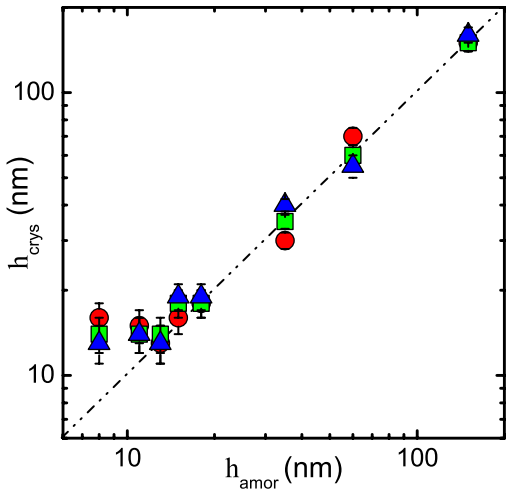

Figure 6. Maximum height of crystalline structures (h_{crys}) on thin films of PLLA isothermally crystallized for 24 h at 358 K (red circles), 373 K (green squares) and 393 K (blue triangles) as a function of its original as casted thickness (h_{amor})

For thicknesses in the range $15 \leq h \leq 100$ nm, we observed a linear relation, $h_{amor} \sim h_{crys}$, which indicates that the crystalline structures could grow within the whole thickness of the spin coated film, independently of the annealing temperature. However, for $h \leq 13$ nm, the thickness of the annealed samples reaches a constant value, around $h_{crys}^{min} = 14 \pm 2$ nm, regardless of its initial thickness and of the annealing temperature. Taking into account that the monomers located within the first 0.9 ± 0.1 nm from the substrate are irreversibly adsorbed (see Figure 3) and that adsorbed chains cannot crystallize, the value of h_{crys}^{min} should read 13 ± 2 nm. Remarkably, this value corresponds to that reported for lamellar thickness of the PLLA[58]. Because formation of ordered structures thinner than the latter quantity is energetically unfavorable, h_{crys} cannot decrease below this critical size. The invariant T_m observed in the thinnest films seems, consequently, related to the development of crystalline structures of a constant height equal to one lamellar thickness. As presented in figure 2c, ellipsometry measurements showed that when film thickness reached values smaller than $h_c \approx h_{crys}^{min}$, the melting temperature remained constant. This evidence finally verifies our hypothesis h_{crys} (h) ~ x (h), and proves that the thickness dependence of T_m is related to the maximum size achieved by crystalline domains at each considered thickness.

3.4 Vitrification of thin polymer films

The successful determination of T_g, T_{CC} and T_m allowed us to build up parameters related the glass forming ability and glass stability in thin films of PLLA down to 6 nm. A large number of definitions have been introduced to characterize these quantities in inorganic glasses[8, 9]; here, we adopted those providing the most direct physical picture. For the latter, we considered the difference between T_{CC} and T_g, indicating the temperature window in which the polymer can be processed in the rubbery state, *i.e* with reduced elastic modulus and melt viscosity, without incurring in crystallization events that would harden the material.

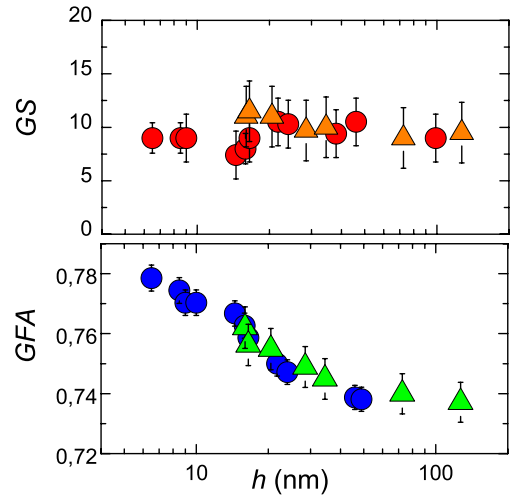

Figure 7. Thickness dependence of the glass stability, GS (T_{CC}-T_g), and glass forming ability, GFA (T_g/T_m)

In the upper graph of figure 7, we plotted the thickness dependence of the glass stability (GS). Within the experimental uncertainty, GS was not affected by confinement, that is, the increase in T_g is balanced by a similar increase in T_{CC}. Reduction of film thickness thus just shifts, but not expands, the temperature window where the glass is stable against devitrification. A similar trend was found by Campoy-Quiles *et al.* when investigating glass transition and cold crystallization

of poly(9,9-dioctylfluorene) and poly(9,9-dioctylfluorene-*co*-benzothiadiazole) during heating scans[14]. On the contrary, in our previous work on 1D confined PLLA[32], we reported extraordinary GS in the time domain, that is, an increase in storage time (t_{cry}) before the onset of crystallization in isothermal conditions, by more than two orders of magnitude. A reduction on the thickness to 15 nm yielded a neat increase by more than 100 folds in t_{cry}[32]. Such an apparent discrepancy is actually in line with our previous reasoning on the impact of a reduction in mass transport on non-equilibrium kinetics. The model proposed by Napolitano *et al.*[39], in fact, verifies that this type of confinement effect is more relevant in experiments performed at constant temperature in the time domain, rather than in temperature scans. In agreement with these ideas, here we verified that large enhancement in GS upon storing at $T>T_g$ is not accompanied by an extension of the processability temperature window.

For the GFA we chose the ratio T_g/T_m, a quantity appearing in several empirical methods to characterize the easiness of a melt to crystallize upon cooling[35]. Alternative formulations of this parameter, including GFA = $(T_{CC}-T_g)/T_m$,[59] would provide a similar trend. Larger T_g/T_m ratios correspond to crystallizing liquids that are less keen to crystallize. In particular, Boyer[60] proposed that $1/2<T_g/T_m<2/3$, with the lower limit corresponding to "symmetric" chains and the upper one to "unsymmetric" polymers (here symmetry indicates the presence of atoms in the main chain bonded to the groups). This correlation relies on the idea that crystallization requires symmetry and that asymmetric compounds are better glass formers.

In the lower panel of Figure 7, we show that for PLLA the T_g/T_m ratio increases upon confinement, reaching at a thickness of 6 nm values 10% higher than in bulk. This trend implies that thinner films form glasses more easily than bulk samples and, in turn, a smaller cooling rate is sufficient to circumvent crystallization upon cooling. The result is not trivial because one might speculate that the presence of interfaces, acting as *contaminants*, speed up heterogeneous nucleation and thus facilitate crystallization upon cooling, as recently observed for PLLA confined in nanopores[61].

On the contrary, as previously mentioned, polymer chains usually crystallize slowly in proximity of interfaces, implying an increase in GFA. Regardless of the trend, the thickness dependence of T_g/T_m confutes, together with several other exceptions, the rule of thumb based on symmetry. To rationalize our findings we analysed the consequences of the increase this fundamental ratio. We considered thickness independent viscosity (η) at any reduced temperature. Similar scaling laws, experimentally observed for the structural relaxation time[62] and the tracer diffusion coefficient[63] support the last hypothesis. Because viscosity exponentially decreases upon heating, an increase in GFA, that is, a reduction in the T_m/T_g, yields a larger viscosity at the melting transition. Via the Stokes-Einstein relation, this condition corresponds to a neat reduction in mass transport (smaller diffusion coefficients) and thus to a smaller crystallization rate and a larger GFA, in line with our reasoning.

Conclusions

The determination of the phase transitions temperatures in thin films of PLLA permitted us to investigate the impact of 1D confinement on vitrification. We observed an increase in glass transition and cold crystallization temperatures upon reduction of the thickness, explained within the framework of the free volume holes diffusion model by the presence of adsorbed layers with suppressed mass transport coefficients. Finally, we found that the thickness dependence of the melting temperature follows that of the maximum extension of crystals in the direction perpendicular to the surface. Analysis of our results highlighted a strong dependence of the glass forming ability on the film thickness supporting the idea that vitrification of polymers is facilitated upon confinement. Remarkably, the increase in T_g/T_m ratio is not accompanied by a larger temperature window where the glassy film does not crystallize upon heating, i.e. bigger $T_{CC}-T_g$ difference, as observed on the contrary, in bulk metallic glasses[59]. We explained this peculiar behavior of soft matter in confinement considering models on the decoupling of time and temperature processes upon confinement.

Acknowledgements

SN acknowledges financial support from the Defay Foundation and the funds FER of the Université LIbre de Bruxelles. AN gratefully acknowledge financial support from the MINECO (MAT2011-23455)

Notes and references

1 1. F. H. Stillinger and P. G. Debenedetti, *Annual Review of Condensed Matter Physics*, 2013, **4**, 263-285.
2 2. P. G. Debenedetti and F. H. Stillinger, *Nature*, 2001, **410**, 259-267.
3 3. L. Larini, A. Ottochian, C. De Michele and D. Leporini, *Nat Phys*, 2008, **4**, 42-45.
4 4. H. Tanaka, T. Kawasaki, H. Shintani and K. Watanabe, *Nat Mater*, 2010, **9**, 324-331.
5 5. E.-J. Donth, *Relaxation and thermodynamics in polymers: glass transition*, Akademie Verlag, 1992.
6 6. When heated above its glass transition, a supercooled liquid will eventually crystallize at the cold crystallization temperature. Such a temperature differs from the melt crystallization temperature, that is, the temperature at which a liquid crystallizes upon cooling below the melting point. While the melt crystallization is governed by nucleation, cold crystallization is, instead, limited by the reduced mass transport in proximity of Tg.

7 7. M. Miller and P. Liaw, *Bulk Metallic Glasses*, Springer, 2008.
8 8. H. X. Li, J. E. Gao, Y. Wu, Z. B. Jiao, D. Ma, A. D. Stoica, X. L. Wang, Y. Ren, M. K. Miller and Z. P. Lu, *Sci. Rep.*, 2013, **3**.
9 9. Z. W. Wu, M. Z. Li, W. H. Wang and K. X. Liu, *Nat Commun*, 2015, **6**.
10 10. B. Vanroy, M. Wübbenhorst and S. Napolitano, *ACS Macro Letters*, 2013, **2**, 168-172.
11 11. O. Guiselin, *EPL (Europhysics Letters)*, 1992, **17**, 225.
12 12. C. Housmans, M. Sferrazza and S. Napolitano, *Macromolecules*, 2014, **47**, 3390-3393.
13 13. J. H. Kim, J. Jang and W.-C. Zin, *Macromolecular Rapid Communications*, 2001, **22**, 386-389.
14 14. M. Campoy-Quiles, M. Sims, P. G. Etchegoin and D. D. C. Bradley, *Macromolecules*, 2006, **39**, 7673-7680.
15 15. J. L. Carvalho, M. V. Massa and K. Dalnoki-Veress, *Journal of Polymer Science Part B: Polymer Physics*, 2006, **44**, 3448-3452.
16 16. H. G. Tompkins and W. A. McGahan, *Spectroscopic Ellipsometry and Reflectometry*, Wiley, 1999.
17 17. K. Fukao and Y. Miyamoto, *Physical Review E*, 2000, **61**, 1743-1754.
18 18. J. A. Forrest and K. Dalnoki-Veress, *Advances in Colloid and Interface Science*, 2001, **94**, 167-195.
19 19. T. Miyata and T. Masuko, *Polymer*, 1998, **39**, 5515-5521.
20 20. B. D. Fitz, D. D. Jamiolkowski and S. Andjelic, *Macromolecules*, 2002, **35**, 5869-5872.
21 21. D. Cava, R. Gavara, J. Lagaron and A. Voelkel, *Journal of Chromatography A*, 2007, **1148**, 86-91.
22 22. J. L. Keddie, R. A. L. Jones and R. A. Cory, *Faraday Discussions*, 1994, **98**, 219-230.
23 23. Y. Grohens, M. Brogly, C. Labbe, M.-O. David and J. Schultz, *Langmuir*, 1998, **14**, 2929-2932.
24 24. D. S. Fryer, P. F. Nealey and J. J. de Pablo, *Macromolecules*, 2000, **33**, 6439-6447.
25 25. C. Zhang, Y. Guo and R. D. Priestley, *Macromolecules*, 2011, **44**, 4001-4006.
26 26. T. Lan and J. M. Torkelson, *Polymer*, 2014, **55**, 1249-1258.
27 27. D. E. Martínez-Tong, J. Cui, M. Soccio, C. García, T. A. Ezquerra and A. Nogales, *Macromolecular Chemistry and Physics*, 2014, **215**, 1620-1624.
28 28. R. D. Priestley, D. Cangialosi and S. Napolitano, *Journal of Non-Crystalline Solids*, 2015, **407**, 288-295.
29 29. Y. Wang, C.-M. Chan, K.-M. Ng and L. Li, *Macromolecules*, 2008, **41**, 2548-2553.
30 30. M. Erber, A. Khalyavina, K. J. Eichhorn and B. I. Voit, *Polymer*, 2010, **51**, 129-135.
31 31. R. S. Tate, D. S. Fryer, S. Pasqualini, M. F. Montague, J. J. de Pablo and P. F. Nealey, *The Journal of Chemical Physics*, 2001, **115**, 9982-9990.
32 32. D. E. Martínez-Tong, B. Vanroy, M. Wübbenhorst, A. Nogales and S. Napolitano, *Macromolecules*, 2014, **47**, 2354-2360.
33 33. D. Cangialosi, V. M. Boucher, A. Alegria and J. Colmenero, *Soft Matter*, 2013, **9**, 8619-8630.
34 34. V. M. Boucher, D. Cangialosi, H. Yin, A. Schonhals, A. Alegria and J. Colmenero, *Soft Matter*, 2012, **8**, 5119-5122.
35 35. J. G. Curro, R. R. Lagasse and R. Simha, *Macromolecules*, 1982, **15**, 1621-1626.
36 36. S. Napolitano and D. Cangialosi, *Macromolecules*, 2013, **46**, 8051-8053.
37 37. S. Napolitano, C. Rotella and M. Wübbenhorst, *Macromolecular Rapid Communications*, 2011, **32**, 844-848.
38 38. S. Napolitano, C. Rotella and M. Wübbenhorst, *ACS Macro Letters*, 2012, **1**, 1189-1193.
39 39. S. Napolitano and M. Wübbenhorst, *The Journal of Physical Chemistry B*, 2007, **111**, 5775-5780.
40 40. R. Lund, A. Alegría, L. Goitandía, J. Colmenero, M. A. González and P. Lindner, *Macromolecules*, 2008, **41**, 1364-1376.
41 41. A. Nogales, T. A. Ezquerra, Z. Denchev and F. J. Baltá Calleja, *Polymer*, 2001, **42**, 5711-5715.
42 42. Y.-X. Liu and E.-Q. Chen, *Coordination Chemistry Reviews*, 2010, **254**, 1011-1037.
43 43. K. Taguchi, H. Miyaji, K. Izumi, A. Hoshino, Y. Miyamoto and R. Kokawa, *Journal of Macromolecular Science Part B*, 2002, **41**, 1033-1042.
44 44. M. Dionísio, M. T. Viciosa, Y. Wang and J. F. Mano, *Macromolecular Rapid Communications*, 2005, **26**, 1423-1427.
45 45. D. Maillard and R. E. Prud'homme, *Macromolecules*, 2008, **41**, 1705-1712.
46 46. X. Wang and R. E. Prud'homme, *Macromolecules*, 2014, **47**, 668-676.
47 47. J.-P. Yang, Q. Liao, J.-J. Zhou, X. Jiang, X.-H. Wang, Y. Zhang, S.-D. Jiang, S.-K. Yan and L. Li, *Macromolecules*, 2011, **44**, 3511-3516.
48 48. Y. Ma, Hu and G. Reiter, *Macromolecules*, 2006, **39**, 5159-5164.
49 49. M. Asada, N. Jiang, L. Sendogdular, J. Sokolov, M. K. Endoh, T. Koga, M. Fukuto, L. Yang, B. Akgun, M. Dimitriou and S. Satija, *Soft Matter*, 2014, **10**, 6392-6403.
50 50. H. Marubayashi, T. Nobuoka, S. Iwamoto, A. Takemura and T. Iwata, *ACS Macro Letters*, 2013, **2**, 355-360.
51 51. Y. Kikkawa, H. Abe, M. Fujita, T. Iwata, Y. Inoue and Y. Doi, *Macromolecular Chemistry and Physics*, 2003, **204**, 1822-1831.
52 52. IUPAC, *Compendium of Chemical Terminology*, Blackwell Scientific Publications, Oxford, 1997.
53 53. Y. Wang, S. Ge, M. Rafailovich, J. Sokolov, Y. Zou, H. Ade, J. Lüning, A. Lustiger and G. Marom, *Macromolecules*, 2004, **37**, 3319-3327.
54 54. Y. Wang, M. Rafailovich, J. Sokolov, D. Gersappe, T. Araki, Y. Zou, A. Kilcoyne, H. Ade, G. Marom and A. Lustiger, *Physical review letters*, 2006, **96**, 028303.

55 55. J. Zhao, X. Yin, J. Shi, X. Zhao and J. S. Gutmann, *The Journal of Physical Chemistry C*, 2011, **115**, 22347-22353.
56 56. F. Zhang, G. G. Baralia, B. Nysten and A. M. Jonas, *Macromolecules*, 2011, **44**, 7752-7757.
57 57. Y. Wang, M. Rafailovich, J. Sokolov, D. Gersappe, T. Araki, Y. Zou, A. D. L. Kilcoyne, H. Ade, G. Marom and A. Lustiger, *Physical Review Letters*, 2006, **96**, 028303.
58 58. D. Maillard and R. E. Prud'homme, *Canadian Journal of Chemistry*, 2008, **86**, 556-563.
59 59. A. Inoue and K. Hashimoto, *Amorphous and Nanocrystalline Materials*, Springer-Verlag Berlin Heidelberg, 2001.
60 60. S. E. Keinath, R. L. Miller and J. K. Rieke, *Order in the Amorphous "State" of Polymers*, Springer, 1987.
61 61. Y. Guan, G. Liu, G. Ding, T. Yang, A. J. Müller and D. Wang, *Macromolecules*, 2015.
62 62. S. Napolitano, V. Lupaşcu and M. Wübbenhorst, *Macromolecules*, 2008, **41**, 1061-1063.
63 63. P. F. Green and E. J. Kramer, *Journal of Materials Research*, 1986, **1**, 202-204.
64

TOC

Confinement strongly improves the glass forming ability of thin films of PLLA